



Energy, Electronic, and Reactivity Descriptors in Quantitative Structure Property Relationships of $[\text{HSO}_4(\text{H}_2\text{O})_n]^-$, $n = 0, 3, 4$

Anant Babu Marahatta^{1,2}

¹Department of Chemistry, Amrit Science Campus, Tribhuvan University, Kathmandu, Nepal

²Department of Civil Engineering, Engineering Chemistry Unit, Kathford International College of Engineering and Management (Affiliated to Tribhuvan University), Kathmandu, Nepal

Corresponding author (e-mail): abmarahatta@gmail.com

Abstract In general, the quantum chemical computations are the most attractive source of quantum-chemical descriptors (QCDs) which in turn are known for their strong abilities to depict all of the electronic and geometric properties of the molecules and their interactions. The quantitative structure property relationship (QSPR) study actually employs them in obtaining optimum structure-property correlations numerically. This work is mainly focused on determining HOMO/LUMO Eigen values and the concerned energy, electronic and reactivity descriptors of the variably sized hydrated bisulfate clusters $[\text{HSO}_4(\text{H}_2\text{O})_n]^-$, $n = 0, 3, \& 4$ separately using DFT: B3LYP hybrid functional method, and on predicting their most significant physicochemical properties quantum mechanically. The major three dimensional structure-based electronic and kinetic properties assessed here are electronegativity, electrophilicity, electronic localization & polarizability, extent of global electron density transfer and chemical hardness & softness. The DFT derived HOMO/LUMO orbital electron densities of each of these ions confirmed the occurrence of electronic delocalization from the central HSO_4^- unit to surrounding H_2O molecules in the course of their structural stabilization. In terms of strength of their nuclear-inbound electron clouds, $[\text{HSO}_4(\text{H}_2\text{O})_4]^-$ cluster is found to have less propensity to loose electrons and has a less polarizable type electron cloud, and in reference to the difference in their chemical potentials, the electron density flux transferring rate is predicted as $[[\text{HSO}_4(\text{H}_2\text{O})_0]^- \text{ to } [\text{HSO}_4(\text{H}_2\text{O})_3]^-] < [[\text{HSO}_4(\text{H}_2\text{O})_3]^- \text{ to } [\text{HSO}_4(\text{H}_2\text{O})_4]^-]$. Meanwhile, the DFT based chemical hardness/softness indices of them indicated the least kinetic stability of $[\text{HSO}_4(\text{H}_2\text{O})_4]^-$ among the ions with $n < 4$.

Keywords Hydrated bisulfate ions, Electronic polarizability, HOMO/LUMO, and QSPR

1. Introduction

The quantitative structure property relationship (hereafter, QSPR) is a powerful analytical and a predictive molecular based research approach that links physicochemical properties of the molecular or ionic specimens mathematically with their 3D structures [1], [2]. It is very often used in finding out quite short yet reliable searching route while investigating unique and functionalized characteristic features of the most desirable and suitable molecular structures. Its primary strategy is to acquire optimum quantitative structure-property correlations simply by employing those quantum-chemical descriptors (hereafter, QCDs) that are derived from the properties of the molecules determined through quantum mechanical calculations. Since such type QCDs encode structural features numerically, they can be employed directly to predict most significant structure activity/property interrelationships



and molecular kinetic stability quantitatively [3]. More important is the QCDs can be used to derive most significant molecular physicochemical properties such as electronic localization & polarizability, electronegativity, electrophilicity, degree of chemical hardness & softness etc. Basically, they are those electronic/geometric properties of the molecular specimens that are based on the electronic descriptors encoding the most reliable quantum information extracted through molecular orbitals' interactions [4], [5]. These descriptors are (1) Energy descriptors: E_{HOMO} and E_{LUMO} (energy of the highest (lowest) occupied (unoccupied) molecular orbital) approximate molecular stability, electronic transition frequency & band gap ΔE_{gap} (HOMO–LUMO energy $\Delta E_{gap} = E_{LUMO} - E_{HOMO}$), and ΔE_{gap} itself indicates how intensely the molecular specimens take part in chemical reactions (larger ΔE_{gap} always means slower electron donation from HOMO to LUMO and vice versa); (2) Electronic descriptors: ionization potential (IP), electron affinity (EA), electronegativity (χ), electronic chemical potentials (μ), and electrophilicity index (ω) describe molecular electronic polarizability and drift velocity; and (3) Reactivity descriptors: chemical-softness (σ) and hardness (η) indicate kinetic stability or molecular reactivity of the reacting specimens [6], [7], [8], [9], [10], [11], [12].

While computational methods based on classical or quantum-mechanical force fields are just useful for determining low energy electronic structures, thermodynamic stabilities, and dipole moments of the molecular specimens, the molecular orbitals (MOs) based quantum-chemical methods are widely used to compute aforementioned descriptors (1), (2), and (3). The density functional theory (hereafter, DFT) is one of them. Quantum mechanically, it is an LCAO-Kohn-Sham ansatz based theoretical model in relation with the spatially dependent electron density function [13], [14], [15]. It is one of the most potential theoretical methods in investigating low energy electronic structures of the many-body-multi-electron molecular/ionic systems as well as in determining MOs, HOMO–LUMO interactions, E_{HOMO} and E_{LUMO} with their proper theoretical quantization [16], [17], [18], [19], [20], [21], [22], [23]. In this study, the DFT method with B3LYP hybrid functional is employed computationally and computed HOMO–LUMO orbitals and their respective Eigen values for the variably sized hydrated bisulfate clusters $[\text{HSO}_4(\text{H}_2\text{O})_n]^-$, $n = 0, 3$, and 4 separately followed by the mathematical determination of ΔE_{gap} and the numerical indices of the most significant QCDs. The main objective of this QSPR study is to interpret experimentally observed: (1) water gaining: $[\text{HSO}_4(\text{H}_2\text{O})_{n-1}]^- + \text{H}_2\text{O} \rightarrow [\text{HSO}_4(\text{H}_2\text{O})_n]^-$; charge separation: $[\text{HSO}_4(\text{H}_2\text{O})_n]^- + \text{H}_2\text{O} \leftrightarrow [\text{SO}_4(\text{H}_2\text{O})_n]^{2-} + \text{H}_3\text{O}^+$; proton gaining (water losing): $[\text{HSO}_4(\text{H}_2\text{O})_n]^- + \text{H}_3\text{O}^+ \leftrightarrow \text{H}_2\text{SO}_4 + (n+1)\text{H}_2\text{O}$ events of the hydrated bisulfate ions [24], [25] in reference to $[\text{HSO}_4(\text{H}_2\text{O})_n]^-$, $n = 0, 3$, and 4, and to understand their (2) electron losing/gaining tendencies in chemical reactions, (3) electron cloud firmly-holding ability, (4) degree of chemical softness/hardness, and (5) electronic polarizability and electrophilicity quantitatively. This in-depth quantum mechanical investigations of their most probable activities in aqueous type solutions may eventually reveal quite essential characteristic features that would eventually be highly useful not only to climatology for illuminating their reactivity and growth mechanisms at vapor/solution interface of aqueous tropospheric aerosols but also to human physiology for explaining various physiological activities and roles in different types of body fluids and to electrochemistry for understanding electrochemical activities of the batteries operated through sulfate and bisulfate enriched aqueous electrolytes.

Actually, the ubiquity of HSO_4^- ion in wide range of aqueous systems is due to its effective dissolution in aqueous systems: polar H_2O molecules surround HSO_4^- ions centrally forming polarized hydration shells $[\text{HSO}_4(\text{H}_2\text{O})_n]^-$ with hydration number n varies from 1 to 16 as reported elsewhere through IR and MS spectroscopies [26]. This hydration phenomenon is most commonly observed in atmospheric aqueous aerosols where significant SO_2 conversion reactions into SO_4^{2-} take place, which exists as $[\text{HSO}_4(\text{H}_2\text{O})_n]^-$ or hydrated H_2SO_4 depending upon the pH level [27]. Similarly, the HSO_4^- ionic hydration and its hydrated complexes exist abundantly in biological systems where they function as denaturing agents to native structure of α -chymotrypsin [28] and as easing specimens to gastrointestinal absorption and metabolic processes plus biosynthetic processes of active sulfate (3'-phosphoadenosine-5'-phosphosulfate (PAPS)) [29]. Moreover, the variably sized hydrated HSO_4^- ions present in the catholyte and anolyte solutions of the electrochemical systems such as redox flow battery technology where aqueous H_2SO_4 is most commonly used as a supporting electrolyte $(\text{H}_2\text{SO}_4(aq.) \leftrightarrow \text{H}^+(aq.) + \text{HSO}_4^-(aq.) \leftrightarrow 2\text{H}^+(aq.) +$



SO_4^{2-} (*aq.*) are involved in conducting electricity [30]. However, the sequential hydration mechanisms of the HSO_4^- ions and their variably sized hydrated complexes are reported as undesirable phenomena due to their adverse effect in electrochemical activity of the lead acid battery system where concentration range of aqueous H_2SO_4 (working electrolyte) is 0.05M to 6.0M [31]. More important is a substantial amount of hydrated HSO_4^- ions are detected in the kitchen vegetables belonging to cruciferous family such as Cauliflower, Broccoli, Chinese cabbage, Chinese broccoli, and many other similar green leaves vegetables [32]. Quantitatively, they are estimated in the range of picomolar (10^{-12} mol/L) level in various ordinary eatable plants, foods, drugs, and many other real-life samples that are predominantly aqueous in nature [33]. Despite all these abundances and necessities of the hydrated HSO_4^- ions in wide range systems, very limited research reports concentrated to the most significant QCDs based QSPR studies are published. In regard to this, current study is intended to derive the most potential QCDs through DFT based computational approach and to employ them for the quantitative prediction of the most significant physicochemical properties and the kinetic stabilities of $[\text{HSO}_4(\text{H}_2\text{O})_n]^-$, $n = 0, 3, \& 4$. Apart from this, the DFT based mathematical indices of the QCDs are used here to interpret the most probable change in physicochemical properties of the hydrated ions in respect to their hydration number n . The structure of this paper is organized as: the computational details are expressed in section 2, the results and discussions are presented in section 3, and the conclusions are given in section 4.

2. Computational Details

As explained in introduction section, the QSPR analyses always access different types of the QCDs enabling to encode structural features of the molecular specimens quantitatively. This is why, the quantum mechanical computation of the fundamental energy descriptors such as E_{HOMO} , E_{LUMO} and ΔE_{gap} is mandatory prior to determine other types of the QCDs. Since this QCDs based QSPR study focuses mainly on the prediction of the most probable characteristic features of the hydrated HSO_4^- ions in reference to $[\text{HSO}_4(\text{H}_2\text{O})_n]^-$, $n = 0, 3, \& 4$ specimens quantum mechanically, the MOs based DFT method with B3LYP hybrid functional is applied here as a computational model to each individual trial structures separately, and computed their low energy electronic structures with frontier MOs such as HOMO, HOMO-1, LUMO, LUMO+1 and their respective Eigen values E . While constructing their trial structures, the molecular structure of HSO_4^- ion was computationally modeled in the *Gaussian* graphical interface *GaussView* [34], and $n\text{H}_2\text{O}$ molecules ($n = 3, 4$) were added one at a time to its immediate vicinity and were made sure that no central and peripheral hydrogen bonding between them takes place. All the Cartesian coordinates of the atoms of each trial structure were extracted and used separately as a *Gaussian* input file for the energy minimization computational procedures. The required *Gaussian* keywords and methodologies were selected as per the instructions mentioned in *Gaussian 09* manual [35]. The standard basis set of the type 6-31G (d, p) was used, where "6-31G" represents the split-valence double-zeta type mathematical functions that describe core and valence orbitals of the atoms; and the function inside the parentheses "(d, p)" indicates polarization type mathematical functions on hydrogen and heavy atoms for describing their chemical bonding. Accordingly, while routing *Gaussian* script for the desirable computations, the separate integral values for ionic charge and spin multiplicity were specified in the *Gaussian* format (charge, spin multiplicity). Here, both hydrated ($n = 3 \& 4$) and unhydrated ($n = 0$) HSO_4^- ions are anionic with a unit negative charge: $[\text{HSO}_4(\text{H}_2\text{O})_n]^-$, $n = 0, 3, \& 4$ has a charge unit of -1 each with spin multiplicity 1, the set of integers used in their respective *Gaussian* input files were $(-1, 1)$. Moreover, the self-consistent field (hereafter, SCF) with both default SCF procedure (SCF=Tight) and Berny algorithm for geometry optimizations to a local minimum were selected [35], [36] for the iterative solution of the electronic Schrodinger equation. Since the current objective of this study is to predict various physicochemical properties of the differently sized hydrated bisulfate clusters through QCDs based QSPR approach, the numerical indices for the most significant descriptors such as ionization potential (IP), electron affinity (EA), chemical hardness (η), chemical softness (σ), electronic chemical potentials (μ), electrophilicity (ω), and electronegativity (χ) were determined numerically using DFT derived Eigen values E_{HOMO} , E_{LUMO} , and their difference ΔE_{gap} as per their mathematical formulations mentioned in equations (Eqs.1-7). While extracting these



basic energy descriptor values, the *Gaussian* output files (such as *.log*, and *.fchk*) of each of the hydrated ions containing three dimensionally displayed chemical data were read through *GaussView*, and the concerned molecular orbitals with HOMO–LUMO surface plots and Eigen values plus molecular electronic configurations were displayed in the 3D space.

3. Results and Discussions

3.1 Importance of Quantum Chemical Descriptors (QCDs)

Despite the inabilities of QCDs in addressing bulk effects directly [37], the QSPR approach is assumed to be a quite significant technique due to their unique mathematical indices that can be utilized to explain structure–property correlations quantitatively. While experimentally measured descriptors are less reliable to elucidate structure activity/property correlations precisely, the quantum mechanically derived descriptors predict comparatively more accurate physicochemical properties as the latter is developed through computational coding without any internal mathematical error (except the minor assumptions made in the quantum mechanical formulations) [1], [2], [3], [5], [23], [37]. In QSPR study, the mostly employed QCDs listed below have direct mathematical relations with computationally derived energy descriptors E_{HOMO} , E_{LUMO} , and ΔE :

$$IP = -E_{HOMO} \quad (1)$$

$$EA = -E_{LUMO} \quad (2)$$

$$\chi = \frac{(IP+EA)}{2} \quad (3)$$

$$\eta = \frac{(-E_{HOMO} + E_{LUMO})}{2} = \frac{\Delta E_{gap}}{2} \quad (4)$$

$$\sigma = \frac{1}{\eta} \quad (5)$$

$$\mu = -\frac{(I+EA)}{2} = -\chi \quad (6)$$

$$\omega = \frac{\mu^2}{2\eta} \quad (7)$$

The Eigen values E_{HOMO} , E_{LUMO} of the two spatially delocalized MOs at the frontier part of the molecular specimens: HOMO and LUMO, and the orbital type HOMO–LUMO interactions not only plays important roles in predicting kinetic molecular stability, but also provides primary information required for describing intramolecular HOMO–LUMO charge transfer events and the related electronic transition frequencies. In addition to this, the HOMO–LUMO orbital interactions and their energy gap (ΔE_{gap}) are used to predict the degrees of hardness, softness, and electronic polarizabilities of the molecular/ionic specimens. The computationally derived three dimensional surface plots of these two frontier MOs and the concerned HOMO–LUMO energy gaps (ΔE_{gap}) for the differently sized hydrated bisulfate ion clusters $[\text{HSO}_4(\text{H}_2\text{O})_n]^-$, $n = 0, 3, \& 4$ plus their mathematical relations with other QCDs are discussed below separately.

3.2 HOMO–LUMO Energy and Energy gap (ΔE_{gap})

This QSPR study targeted to predict most significant physicochemical properties of the variably sized hydrated bisulfate ions $[\text{HSO}_4(\text{H}_2\text{O})_n]^-$, $n = 0, 3, \& 4$ needs their DFT produced HOMO–LUMO surface plots, and the respective Eigen values E_{HOMO} and E_{LUMO} while determining other major type of the QCDs mathematically. The concerned electron density based surface plots of these frontier MOs of each of the HSO_4^- ions are displayed in Figure 1 to Figure 3 respectively, where calculated values of the energy gaps ΔE_1 , ΔE_2 , and ΔE_3 in both *Hartree* (*a.u.*) and *Electron Volt* (*eV*) units are clearly mentioned. As can be seen in Figure 1, the HOMO electron density surface of unhydrated HSO_4^- ion ($n = 0$) is mainly distributed over the four O atoms while the LUMO surface is distributed over the entire ionic specimen.

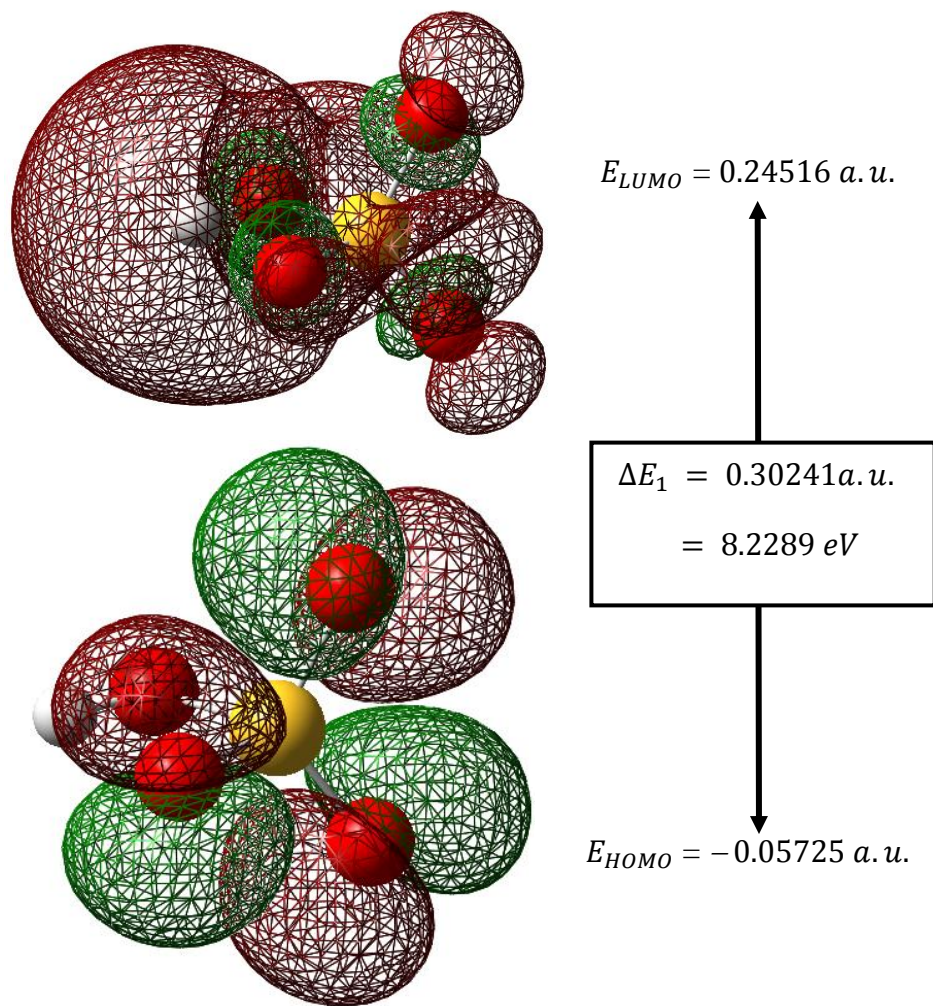


Figure 1: DFT computed surface plots of HOMO and LUMO depicting HOMO–LUMO energy gap ΔE_1 for $[\text{HSO}_4(\text{H}_2\text{O})_0]^-$ ion.

In the case of trihydrated HSO_4^- ion with $n = 3$, the HOMO surface is highly localized over the central HSO_4^- unit while the LUMO surface shows a significant probability electron density over the hydrated H_2O molecules, but in the hydrated state with $n = 4$, both HOMO and LUMO surfaces are localized centrally around HSO_4^- unit as can be seen in Figure 3. This variation of the electronic occupancy in the frontier molecular orbitals not only highlights the existence of electronic delocalization from the central HSO_4^- unit to surrounding H_2O molecules during the course of structural stabilization as reported elsewhere [21] by the same author but also verifies the optical electronic excitation (HOMO to LUMO transition) phenomena shown by the HOMO electron.

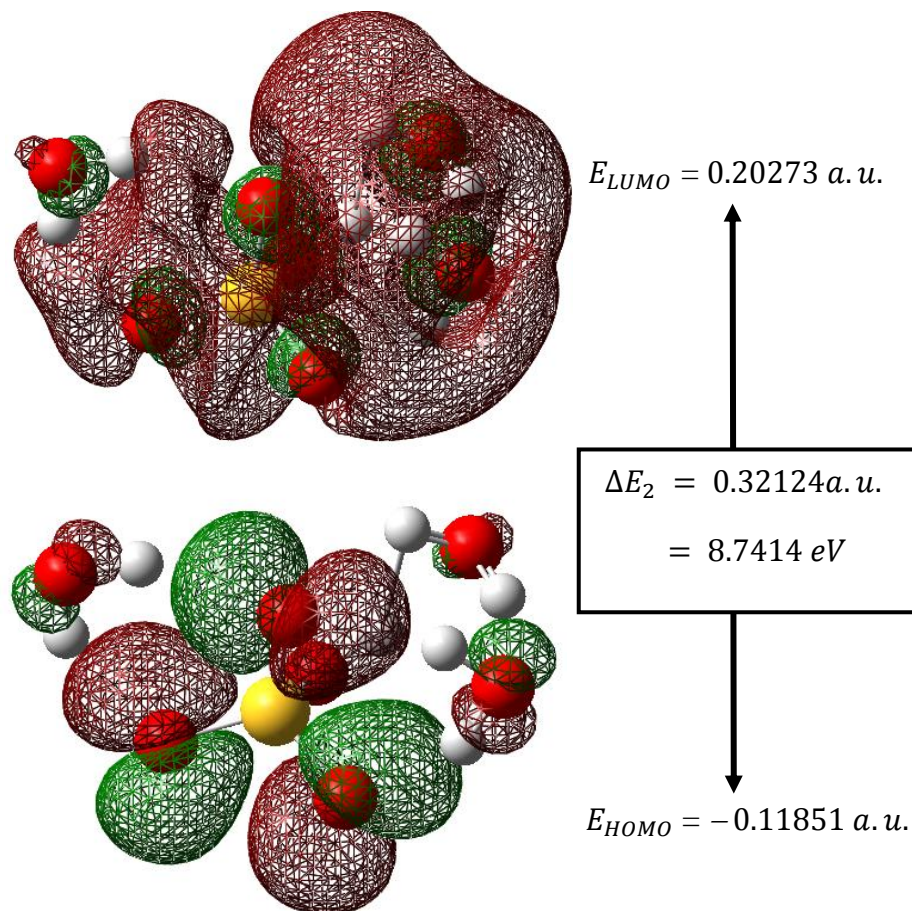


Figure 2: DFT computed surface plots of HOMO and LUMO depicting HOMO–LUMO energy gap ΔE_2 for $[\text{HSO}_4(\text{H}_2\text{O})_3]^-$ ion.

If we refer to these electron density surfaces, we may observe asymmetric holes on all the LUMO surfaces, indicating the origination of attractive force that can bind electron cloud more closely to the ionic centers. Moreover, the DFT derived HOMO–LUMO energy gaps $\Delta E_1 = 8.2289 \text{ eV}$, $\Delta E_2 = 8.7414 \text{ eV}$, $\Delta E_3 = 5.8428 \text{ eV}$ for the $[\text{HSO}_4(\text{H}_2\text{O})_n]^-$, $n = 0, 3 \text{ \& } 4$ ions respectively approximates their band gaps (electronic band gaps) exist in between valence band and conductance band and hence, predicts their individual lowest energy transition frequencies in UV visible spectroscopy.

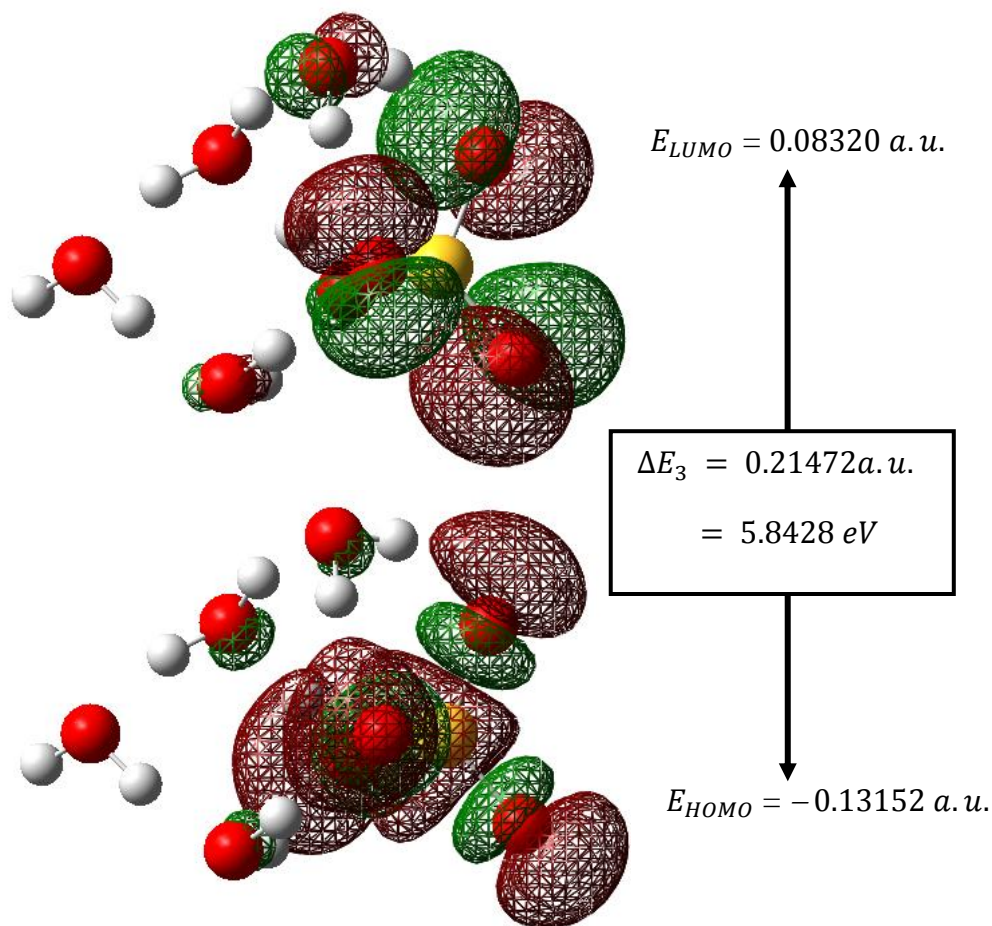


Figure 3: DFT computed surface plots of HOMO and LUMO depicting HOMO–LUMO energy gap ΔE_3 for $[\text{HSO}_4(\text{H}_2\text{O})_4]^-$ ion.

If we compare these values for tri- and tetra- hydrated clusters to each other, the trend is in decreasing order: $\Delta E_2 > \Delta E_3$. It indicates that the HOMO to LUMO electronic transition occurs comparatively more easily with increasing hydration number n , suggesting $[\text{HSO}_4(\text{H}_2\text{O})_4]^-$ cluster is kinetically less stable (smaller ΔE_{gap} always infers lower ionic/molecular stability means higher is the chemical reactivity) even though it is predicted as energetically more stable through theoretical electronic structure calculations [21]. From this observation, it can be generalized that bigger the size of the hydrated bisulfate cluster, higher is the chemical reactivity, exactly similar trend as that of the hydrated sulfate clusters $[\text{SO}_4(\text{H}_2\text{O})_n]^{2-}$ ($n = 1-4, 16$) reported elsewhere [38]. The detailed 3D structure based physicochemical properties (QSPR) of these variably sized hydrated bisulfate ion clusters can only be predicted through the quantitative analysis of quantum mechanically determined QCDs as explained below concisely.

3.3. Quantum-Chemical Descriptors (QCDs) in QSPR analysis

Since the quantum-chemical (mechanical) descriptors in QSPR analysis are very often used to depict some of the most significant physicochemical properties of the molecular/ionic specimens numerically, they are widely known as typical type global numerical indicators. These indicators are actually used to provide quantum mechanical insights into the most appropriate molecular/ionic properties which in turn are highly associated with their structure

based activities (QSAR). In the following subsections, a brief explanation of the concerned molecular descriptors (Table 1.) and their uses in featuring structure property/activity correlations are presented in reference to the variably sized hydrated bisulfate ion clusters $[\text{HSO}_4(\text{H}_2\text{O})_n]^-$ with $n = 0, 3 \text{ \& } 4$.

Table 1: A DFT computed quantum chemical descriptors (QCDs) for the hydrated bisulfate clusters $[\text{HSO}_4(\text{H}_2\text{O})_n]^-$, $n = 0, 3, \text{ \& } 4$.

| QCDs (eV) | Hydrated bisulfate ions | | |
|------------------|--|--|--|
| | $[\text{HSO}_4(\text{H}_2\text{O})_0]^-$ | $[\text{HSO}_4(\text{H}_2\text{O})_3]^-$ | $[\text{HSO}_4(\text{H}_2\text{O})_4]^-$ |
| E_{HOMO} | -1.5578 | -3.2248 | -3.5788 |
| E_{LUMO} | 6.6711 | 5.5165 | 2.2640 |
| ΔE_{gap} | 8.2289 | 8.7414 | 5.8428 |
| IP | 1.5578 | 3.2248 | 3.5788 |
| EA | -6.6711 | -5.5165 | -2.2640 |
| χ | -2.5566 | -1.1458 | 0.6574 |
| μ | 2.5566 | 1.1458 | -0.6574 |
| ω | 0.7943 | 0.1502 | 0.0740 |
| η | 4.1144 | 4.3707 | 2.9214 |
| σ | 0.2430 | 0.2288 | 0.3423 |

3.3.1. Electronic Descriptors

The descriptors that are associated with the electronic structures, and their corresponding energy descriptors E_{HOMO} , E_{LUMO} , and ΔE obtained through the series of MOs based quantum mechanical computations are called electronic descriptors. Following are the most important 3D structure based descriptors employed here to depict electronic polarizabilities and the related consequences of the hydrated bisulfate clusters $[\text{HSO}_4(\text{H}_2\text{O})_n]^{2-}$, $n = 0, 3 \text{ \& } 4$.

(1) Ionization Potential (IP)

In any molecular or ionic specimens, the electrons are held centrally through the positively charged nucleus. This electron-nucleus binding force can be measured by an electronic descriptor called ionization potential (hereafter, IP). It is a parameter that quantitatively approximates the amount of energy required to remove most loosely bound electron out of the nuclear territory from the isolated molecular or ionic specimens in their ground electronic states [39], [40]. Thus, it is an endothermic type energy whose absolute value can be taken as a mathematical index to approximate the strength of the chemical bonds. In QSPR analysis, its quantum mechanically derived mathematical index is used as a parameter while predicting kinetic stability of the molecular or ionic specimens. The principle behind this is molecules or ions having less-tightly held electrons would have comparatively low IP values and hence, they may have high tendency of behaving as good reducing agents (high propensity of losing electrons or undergoing oxidation) and of generating corresponding cationic forms more likely. It eventually explains that such molecules or ions are comparatively more reactive, less kinetically-stable/chemically-inert, and have high susceptibility towards electrophilic attack. In theoretical computations, this descriptor is mathematically related to the quantum mechanically derived Eigen values E_{HOMO} , E_{LUMO} (Eq.1). The absolute numerical values of it (eV) for the variably sized hydrated bisulfate clusters $[\text{HSO}_4(\text{H}_2\text{O})_n]^-$, $n = 0, 3, \text{ \& } 4$ are summarized in Table 1. If we compare the magnitude of their IP, the order is: $[\text{HSO}_4(\text{H}_2\text{O})_4]^- > [\text{HSO}_4(\text{H}_2\text{O})_3]^- > [\text{HSO}_4(\text{H}_2\text{O})_0]^-$. It means, among these clusters, the ion with $n = 4$ has less propensity to loose electrons or to produce its cationic form than that with $n = 3$ ion. It suggests that $[\text{HSO}_4(\text{H}_2\text{O})_4]^-$ ion has comparatively more tightly held plus less polarizable type electron cloud. From this, it can be approximately generalized that bigger the size of the hydrated bisulfate clusters, more is the nuclear-inbound electron cloud. And, this is a quite explanatory result because the electrons of the centrally located bisulfate ion are more delocalized to the surrounding H_2O molecules that eventually results a creation of the stronger hydrogen bonded network between themselves.



(2) Electron Affinity (EA)

In contrary to *IP*, the "Electron Affinity" (*EA*) is an exothermic type energy that is released while adding an extra electron to the atom of isolated molecules/ions in the ground state [41]. It actually evaluates the intensity of accepting an electron by the isolated ionic or molecular specimens. The theoretically derived absolute value of it is very often used while predicting oxidizing/reducing abilities of the molecules/ions and characterizing their susceptibility towards nucleophilic attack. More especially, in charge-transfer reactions, the numerical index of *EA* is used to identify electron accepting or donating behavior of the molecular/ionic specimens: those having more or less *EA* values tend to behave as good electron acceptor or donor respectively. If we refer to the *EA* values (magnitude) of the hydrated bisulfate clusters listed in Table 1, the trend is $[\text{HSO}_4(\text{H}_2\text{O})_4]^- < [\text{HSO}_4(\text{H}_2\text{O})_3]^- < [\text{HSO}_4(\text{H}_2\text{O})_0]^-$, implying that the unhydrated bisulfate ion has a more affinity for the electrons than that with other hydrated ions. This is as per our well-established principle: more negative *EA* value always infers higher affinity of the atoms towards the electrons. Alternatively, among the clusters with $n < 4$, $[\text{HSO}_4(\text{H}_2\text{O})_4]^-$ ion ($n = 4$) has a relatively lower affinity for the electrons due to having the least negative *EA* value, further indicating that $[\text{HSO}_4(\text{H}_2\text{O})_4]^-$ ion is comparatively not good at accepting extra electrons. The similar type explanations could be valid to the clusters with $n > 4$ which is, however, not sampled here due to the unavailability of the computational resources. As a whole, this quantitative prediction of the comparatively higher electron-accepting propensities of the hydrated bisulfate clusters with $n < 4$ supports the fact that " $[\text{HSO}_4(\text{H}_2\text{O})]^-$ and $[\text{HSO}_4(\text{H}_2\text{O})_2]^-$ ions do not exist in the aqueous type solutions" as they are highly unstable species and always tend to stabilize through the sequential hydration step by step (gain of H_2O molecules: $[\text{HSO}_4(\text{H}_2\text{O})_{n-1}]^- + \text{H}_2\text{O} \rightarrow [\text{HSO}_4(\text{H}_2\text{O})_n]^-$) during which intense distribution of atomic charges from the central HSO_4^- unit to immediate H_2O molecules occurs.

(3) Electronegativity (χ)

Electronegativity is that type of the electronic indicator used in QSPR studies which enables quantum chemists to approximate tendency of attracting shared electron pair towards bonded atoms or group of atoms of the molecules or ions [41]. This parameter is actually affected by the distance that the valence electrons reside from the positively charged nuclei. More specifically, the Mulliken introduced concept of absolute electronegativity (the arithmetic mean of *IP* and *EA* as shown in Eq. 3) can be used to identify the polar region/s of the molecule: higher electronegativity value always signifies stronger intensity of an atom or a substituent group to create oppositely charged terminals. In the chemical reactions, the difference in electronegativity $\Delta\chi = \chi_2 - \chi_1$ of the two reacting specimens always plays vital role: a specimen of lower electronegativity (χ_1) transfers electrons to another specimen of higher electronegativity (χ_2) until they attain equal electronegativity values (Electronegativity Equalization Principle (EEP)). In the reaction between electron acceptor (Lewis acid "A") and electron donor (Lewis base ":B"), an EEP measures the quantity of charge transfer ΔN and the energy change ΔE associated with the reaction that results A:B type complex product [39]. In a conceptual analogy of the same, we may predict the electron transferring/accepting abilities of the hydrated bisulfate clusters in their possible chemical reactions. As listed in Table 1, $[\text{HSO}_4(\text{H}_2\text{O})_4]^-$ ion has the highest χ value among the clusters with $n < 4$, indicating that former may accept electrons transferred by the latter type clusters, further supporting the fact that $[\text{HSO}_4(\text{H}_2\text{O})_4]^-$ ion has comparatively more tightly held plus less polarizable type electron cloud as depicted by its *IP* value presented in subsection 3.3.1(1).

(4) Electronic Chemical Potential (μ)

It is that type of the electronic descriptor which in principle measures escaping tendency of the electronic cloud from one ionic/molecular specimen to another whenever they mutually combine in the ground electronic state conditions [42]. The driving force for this electronic fleeing propensity is the difference in chemical potential (μ) between any two reacting specimens 'Y' and 'Z'. If μ_Y and μ_Z represent their respective electronic chemical potentials, and $\mu_Y > \mu_Z$, the electronic cloud of 'Y' fluxes towards 'Z' until this interacting chemical system achieves equilibrated electronic chemical potential μ_{YZ} . Here, these two reacting specimens 'Y' and 'Z' behave as electron-donor or nucleophile and



electron-acceptor or electrophile respectively. Mathematically, μ is equal to negative of the electronegativity (χ) in Mulliken and Pauling scale (Eq. (6)). In quantum mechanics, the absolute value of it can be used to interpret electronic polarizability of the interacting molecular/ionic specimens: lower value of μ depicts easier electron gaining (or difficult to lose) or the presence of more tightly held electron cloud in molecular/ionic specimens. More importantly, the difference in the chemical potentials $\Delta\mu$ ($\mu_Y - \mu_Z$) of 'Y' and 'Z' approximates the extent of global electron density transfer (GEDT) in polar chemical reactions [43]. As an example, the significantly low $\Delta\mu$ ($\Delta\mu = \mu_1 - \mu_2$) values for the ionic pairs: (1) $[\text{HSO}_4(\text{H}_2\text{O})_0]^-$ and $[\text{HSO}_4(\text{H}_2\text{O})_3]^-$ ($\Delta\mu = 1.41$ eV), and (2) $[\text{HSO}_4(\text{H}_2\text{O})_3]^-$ and $[\text{HSO}_4(\text{H}_2\text{O})_4]^-$ ($\Delta\mu = 1.80$ eV) signify that the GEDT between them is relatively small. These $\Delta\mu$ values eventually depict electron density flux transferring rate between the concerned ionic pairs which is found to be in the order $[[\text{HSO}_4(\text{H}_2\text{O})_0]^- \text{ to } [\text{HSO}_4(\text{H}_2\text{O})_3]^-] < [[\text{HSO}_4(\text{H}_2\text{O})_3]^- \text{ to } [\text{HSO}_4(\text{H}_2\text{O})_4]^-]$. From this, we may predict that these ionic pairs must undergo electron/charge transfer reactions [44] between themselves as depicted above from their respective χ values which is, however needs more trustworthy experimental and theoretical verifications to establish the fact.

(5) Electrophilicity Index (ω)

Parr *et al.* [42] has defined Electrophilicity index (ω) as a parameter that can measure energy lowering associated with the maximum electron flow from the donor to acceptor specimens. In another words, it approximates the tendency of acceptor molecular/ionic specimens to gain an additional electronic charge from the similar donor type specimen. Therefore, this parameter estimates the electron-loving or electrophilic ability of the molecular/ionic specimens quantitatively. The same feature of this descriptor has actually made it a quite significant quantum mechanical index in an electrophile-nucleophile chemistry more especially for interpreting electrophilicity of the most of the interacting organic specimens and their chemical reactions. According to the quantum mechanical perspective, it is formulated with the square of the chemical potential (μ^2), and chemical hardness (η) as shown in Eq. (7). This mathematical relationship is very often used to identify the specimens having most intense electrophilic abilities: those having higher value of μ^2 , but lower value of η must have relatively higher value of ω , indicating themselves as the most electron-loving specimens.

The DFT derived values of η and ω for the variably sized hydrated bisulfate ion clusters $[\text{HSO}_4(\text{H}_2\text{O})_n]^-$, $n = 0, 3$ & 4 are listed in Table 1. The relatively higher values of μ , and ω but comparable value of η for $[\text{HSO}_4(\text{H}_2\text{O})_0]^-$ ion ($\mu = 2.5566$ eV, $\omega = 0.7943$ eV, $\eta = 4.1144$ eV) than those for $[\text{HSO}_4(\text{H}_2\text{O})_3]^-$ ($\mu = 1.1458$ eV, $\omega = 0.1502$ eV, $\eta = 4.3707$ eV) indicates that the former ion has comparatively higher degree of electrophilicity or stronger electrophilic character (difficult (easy) to lose (gain) electron) than the latter and accordingly, the last ion with $n = 4$; $[\text{HSO}_4(\text{H}_2\text{O})_4]^-$ ($\mu = -0.6574$ eV, $\omega = 0.0740$ eV, $\eta = 2.9214$ eV) has the least degree of electron loving tendency among the clusters with $n < 4$. This is because former type ions are in the state of changing more stable clusters *via* the association of additional H_2O molecules, but the latter ion is already more stabilized through the peripheral addition of four H_2O molecules. In fact, H_2O is an electron rich nucleophile whose central O atom is highly polar with two lone pair electrons and is involved in hydrogen bonding with the central HSO_4^- unit in the course of structural stabilization of each hydrated cluster. Thus, in general, all these bisulfate clusters with $n \leq 4$ may show high preference towards electron rich terminal of H_2O , demonstrating their propensity in making bigger and bigger hydrated clusters through step-by-step hydration mechanism: $[\text{HSO}_4(\text{H}_2\text{O})_{n-1}]^- + \text{H}_2\text{O} \rightarrow [\text{HSO}_4(\text{H}_2\text{O})_n]^-$. The detailed averaged *Gibbs* free energy change (ΔG) during such stepwise H_2O addition mechanism is reported by Tsona *et al.* elsewhere [24]. Moreover, the charge separation reaction of the HSO_4^- ion ($[\text{HSO}_4(\text{H}_2\text{O})_n]^- + \text{H}_2\text{O} \leftrightarrow [\text{SO}_4(\text{H}_2\text{O})_n]^{2-} + \text{H}_3\text{O}^+$) transforming into SO_4^{2-} and H_3O^+ is governed by the variation in their hydration strength: the products SO_4^{2-} and H_3O^+ interact relatively more strongly than that in between HSO_4^- and H_2O favoring forward reaction [44], reassuring again the same type of sequential hydration mechanisms of the HSO_4^- ion.



3.3.2. Reactivity Descriptors

(1) Chemical Hardness (η) and Chemical Softness (σ)

A qualitative concept for Hard and Soft Acids and Bases (HSAB principle) introduced by R. G. Pearson in 1963 has been realized fully as a fundamental tool to characterize and classify Lewis acids and Lewis bases type molecular compounds into hard or soft or borderline types. It is actually based on frontier molecular orbital (FMO) analysis plus HOMO–LUMO interactions [45]. According to this analysis, the Lewis acid-base type interactions are mainly governed by the relative energies of HOMO (E_{HOMO}), LUMO (E_{LUMO}), and their energy gap (ΔE). The closely associated terminologies of the Hard and Soft category of Lewis acids and Lewis bases with those FMO's energy parameters are chemical hardness (η) and chemical softness (σ) respectively. These descriptors are actually used to quantize the electronic polarizability of the interacting chemical species. Literally, the term "Hard" refers to those chemical species that are characterized by small ionic size, high charge density, non-polarizable electron cloud, and high preference of participation in ionic bonding interactions whereas "Soft" applies to those which have low charge density and are large and strongly polarizable. The quantum mechanically derived η , and σ indices enable chemists/physicists to predict kinetic stabilities or chemical reactivities of any molecular/ionic specimens without referring to large supercomputers and databases. These indices can be computed by using the mathematical equations formulated in Eqs. 4 and 5 in subsection 3.1. In the range of DFT based mathematical scheme, η is defined by the second order derivative of the electronic energy E of any chemical/ionic systems with respect to number of electrons N , *i.e.* for a fixed external potential $V(r)$, η can be expressed in terms of following mathematical relationship:

$$\eta = \frac{1}{2} \left[\frac{\partial^2 E}{\partial N^2} \right] = \frac{1}{2} \left[\frac{\partial \mu}{\partial N} \right] \quad (8)$$

On the basis of this mathematical equation, it can be said that η and its inverse parameter σ measure how intensely the molecular/ionic specimens acquire electrons which further means they describe the chemical reactivity or kinetic stability of the specimens quantitatively. While correlating the concerned energy descriptors E_{HOMO} , E_{LUMO} and HOMO–LUMO energy gap ΔE_{gap} (Figure 1-Figure 3) with η , it can be deduced that smaller (larger) the η (σ) value faster is the electronic transition from HOMO orbital to LUMO orbital suggesting that more reactive the molecular specimens become. In contrast to this, the molecular/ionic specimens possessing smaller (larger) ΔE_{gap} always have low (high) degree of hardness, specifying more (less) reactive or soft (hard) specimens having facile electronic polarizing abilities. Furthermore, the activation hardness of the molecules/ions that is used more especially in differentiating the rates of the reactions occurred at their different reactive sites can also be defined on the basis of ΔE_{gap} . Hence, it is more appropriate while predicting orientation effects of the reacting specimens as well.

The quantum mechanically derived absolute values of the η and σ indicators for the variably sized hydrated bisulfate clusters $[\text{HSO}_4(\text{H}_2\text{O})_n]^-$, $n = 0, 3$ & 4 are listed in Table 1. While comparing η or σ values of these hydrated clusters, one may conclude that greater the hydration number n of the bisulfate ion, lesser (greater) is the degree of chemical hardness (softness). In particular, the biggest hydrated bisulfate ion cluster $[\text{HSO}_4(\text{H}_2\text{O})_4]^-$ sampled in this study has comparatively the lowest value of $\eta = 2.9214 \text{ eV}$ (highest value of $\sigma = 2.9214 \text{ eV}$), suggesting this as a cluster having relatively less (more) degree of chemical hardness (softness) and faster chemical reactivity or least kinetically stability. In respect to electronic polarizability, the relatively harder and less reactive $[\text{HSO}_4(\text{H}_2\text{O})_3]^-$ ion must have restricted electronic polarizations due to the presence of tightly-held electron cloud than in other clusters with $n < 3$. In terms of HOMO to LUMO charge transfer events or chemical reactions, the $[\text{HSO}_4(\text{H}_2\text{O})_4]^-$ state ($\Delta E = 5.8428 \text{ eV}$) has relatively more tendency than $[\text{HSO}_4(\text{H}_2\text{O})_3]^-$ ($\Delta E = 8.7414 \text{ eV}$) due to having low HOMO –LUMO energy gap. This is actually based on the principle that the HOMO electrons are always regarded as the most reactive electrons, and their rapid transition to LUMO determines ionic/ molecular kinetic stability or reactivity quantum mechanically.



4. Conclusion

The QSPR analysis is a quantitative type study known among the scientists for its extraordinary skills of employing several quantum mechanical descriptors that have abilities to code large well-defined physicochemical information. This feature actually enables itself to present these two major advantages: (a) characterization of the compounds and substituents, and (b) prediction of their chemical reactivity or molecular stability in computational molecular designing/modeling and structure entry steps of theoretical chemistry and chemical drug design. The main responsible fundamental part of the QSPR technique behind these notable predictions is a three dimensional structure of the molecules. In this research work, the computationally cheap yet decent hybrid density functional DFT: B3LYP with 6-31G (*d*, *p*) basis set was employed and interpreted the three dimensional structure-property correlations and the concerned QSPR analyses of the variably sized hydrated bisulfate ion clusters $[\text{HSO}_4(\text{H}_2\text{O})_n]^-$, $n = 0, 3, \& 4$ quantitatively. The principal 3D molecular structure based quantum-chemical descriptors (QCDs) accessed in this study were E_{HOMO} , E_{LUMO} , HOMO-LUMO energy gaps (ΔE_{gap}), ionization potential (*IP*), electron affinity (*EA*), chemical hardness (η), chemical softness (σ), electronic chemical potential (μ), electrophilicity index (ω), and electronegativity (χ). While confirming the 3D structural entity and the most significant probability electron density of each ion, the DFT computed surface plots of the molecular orbitals including HOMO and LUMO were thoroughly analyzed. In terms of strength of the HOMO/LUMO nuclear-inbound electron clouds, $[\text{HSO}_4(\text{H}_2\text{O})_4]^-$ cluster was found to have less propensity to loose electrons and has a less polarizable type electron cloud, and in reference to the difference in the chemical potentials $\Delta\mu$, the electron density flux transferring rate was predicted as $[[\text{HSO}_4(\text{H}_2\text{O})_0]^- \text{ to } [\text{HSO}_4(\text{H}_2\text{O})_3]^-] < [[\text{HSO}_4(\text{H}_2\text{O})_3]^- \text{ to } [\text{HSO}_4(\text{H}_2\text{O})_4]^-]$. Meanwhile, while comparing the DFT based chemical hardness/softness indices of them, the $[\text{HSO}_4(\text{H}_2\text{O})_4]^-$ ion was found to be the least kinetically stable among the ions with $n < 4$. To the knowledge of this author, the results presented here are quite reliable, but it is still recommended to use other advanced theoretical models with systematically convergent basis sets [46] for producing more quantitative type structural correlations.

References

- [1]. M. Karelson, V. S. Lobanov, A. R. Katritzky, "Quantum-Chemical Descriptors in QSAR/ QSPR Studies", *Chemical Review*, Vol. 96 (3), pp. 1027–1043, 1996.
- [2]. Peixun Liu, Wei Long, "Current Mathematical Methods Used in QSAR/QSPR Studies", *International Journal of Molecular Sciences*, Vol. 10(5), pp. 1978–1998, 2009.
- [3]. J. Fei, Q. Mao, L. Peng, T. Ye, Y. Yang, S. Luo, "The Internal Relation between Quantum Chemical Descriptors and Empirical Constants of Polychlorinated Compounds", *Molecules*, Vol. 23(11), pp. 2935:1–12, 2018.
- [4]. J. Jaworska, N. Nikolova-Jeliazkova, T. Aldenberg, "QSAR applicability domain estimation by projection of the training set in descriptor space: A review", *Alternatives to Laboratory Animals*, Vol. 33, pp. 445–459, 2005.
- [5]. T. Papp, L. Kollar, T. Kegl, "Employment of quantum chemical descriptors for Hammett constants: Revision Suggested for the acetoxy substituent", *Chemical Physics Letter*, Vol. 588, pp. 51–56, 2013.
- [6]. W. L. Jolly, "*Modern Inorganic Chemistry*", McGraw-Hill Book Company, New York, 1984.
- [7]. E. C. Koch, "Acid-Base Interactions in Energetic Materials: "I. The Hard and Soft Acids and Bases (HSAB) Principle-Insights to Reactivity and Sensitivity of Energetic Materials", *Propellants, Explosives, Pyrotechnics*, Vol. 30(1), pp. 5–16, 2005.
- [8]. M. S. A. Abdel-Mottaleb, S. N. Ali, "A New Approach for Studying Bond Rupture/Closure of a Spiro Benzopyran Photochromic Material: Reactivity Descriptors Derived from Frontier Orbitals and DFT Computed Electrostatic Potential Energy Surface Maps", *International Journal of Photoenergy*, Article ID 6765805, pp. 1–9, 2016.
- [9]. S. Kumar, A. Syed, S. Andotra, R. Kaur, Vikas, S. K. Pandey, "Investigation of synthesized new vanadium(III) complexes of ditolyldithiophosphate ligands by spectroscopic, cyclic voltammetric, DFT, antimicrobial and cytotoxic studies", *Journal of Molecular Structure*, Vol. 1154, pp. 165–178, 2018.



- [10]. M. Saranya, S. Ayyappan, R. Nithya, R. K. Sangeetha, A. Gokila, "Molecular structure, NBO and HOMO–LUMO analysis of quercetin on single layer graphene by density functional theory", *Digest Journal of Nanomaterials and Biostructures*, Vol. 13, No. 1, pp. 97–105, 2018.
- [11]. T. Abbaz, A. Bendjeddou, D. Villemin, "Molecular orbital studies (hardness, chemical potential, electro negativity and electrophilicity) of TTFs conjugated between 1, 3–dithiole", *International Journal of Advanced Research in Science, Engineering and Technology*, Vol. 5(2), pp. 5150–5161, 2018.
- [12]. T. M. Nolte, W. J. G. M. Peijnenburg, "Use of quantum-chemical descriptors to analyse reaction rate constants between organic chemicals and superoxide/hydroperoxyl ($O_2^{\cdot-}/HO_2^{\cdot}$)", *Free Radical Research*, Vol. 52(10), pp. 1118–1131, 2018.
- [13]. P. Hohenberg, W. Kohn, "Inhomogeneous Electron Gas", *Physical Review B*, Vol. 136, No. 3B, pp. 864–871, 1964.
- [14]. W. Kohn, L. Sham, "Self-Consistent Equations Including Exchange and Correlation Effects", *Physical Review Journal*", Vol. 140, No. 4A, pp. A1133–A1138, 1965.
- [15]. A. B. Marahatta, "A DFT Analysis for the Electronic Structure, Mulliken Charges Distribution and Frontier Molecular Orbitals of Monolayer Graphene Sheet", *International Journal of Progressive Sciences and Technologies*, Vol. 16, No. 1, pp. 51–65, 2019.
- [16]. A. B. Marahatta, "Effect of *n*-Type Dopant Nitrogen in the Structure and Atomic Charges Distribution of Monolayer Graphene Sheet: A DFT Analysis", *International Journal of Progressive Sciences and Technologies*, Vol. 16, No. 2, pp. 01–13, 2019.
- [17]. A. B. Marahatta, "DFT Study on Ground State Electronic Structures of Simple to Complex Molecular Specimens", *International Journal of Progressive Sciences and Technologies*, Vol. 19, No. 1, pp. 100–112, 2020.
- [18]. A. B. Marahatta, H. Kono, "Comparative Theoretical Study on the Electronic Structures of the Isolated Molecular Gyroscopes with Polar and Nonpolar Phenylene Rotator", *International Journal of Progressive Sciences and Technologies*, Vol. 20, No. 1, pp. 109–122, 2020.
- [19]. A. B. Marahatta, "Computational Study on Electronic Structure, Atomic Charges Distribution and Frontier Molecular Orbitals of Butadiene: General Features for Diels-Alder Reaction", *International Journal of Progressive Sciences and Technologies*, Vol. 19, No. 2, pp. 48–64, 2020.
- [20]. A. B. Marahatta, "A DFT Study of Electronic Structures on Hydrated Sulfate Clusters $[SO_4^{2-}(H_2O)_n]$; $n = 0-4, 16$ ", *International Journal of Progressive Sciences and Technologies*, Vol. 17, No. 1, pp. 55–69, 2019.
- [21]. A. B. Marahatta, "Theoretical Study on Microhydration of Bisulfate Ions $[HSO_4^-(H_2O)_n]$, $n = 0-3, 5$ ", *International Journal of Progressive Sciences and Technologies*, Vol. 18, No. 2, pp. 43–53, 2020.
- [22]. R. G. Parr, Y. Weitao, "Density-Functional theory of Atoms and Molecules", Oxford University Press, 1994.
- [23]. A. B. Marahatta, "DFT Study on Electronic Charge Distribution and Quantum-Chemical Descriptors for the Kinetic Stability of Vanadium Aquo Complex Ions $[V(H_2O)_6]^{2+}$ and $[V(H_2O)_6]^{3+}$ ", *International Journal of Progressive Sciences and Technologies*, Vol. 22, No. 1, pp. 67–81, 2020.
- [24]. N. T. Tsona, H. Henschel, N. Bork, V. Loukonen, H. Vehkamäki, "Structures, Hydration, and Electrical Mobilities of Bisulfate Ion–Sulfuric Acid–Ammonia/Dimethylamine Clusters: A Computational Study", *Journal of Physical Chemistry A*, Vol. 119, pp. 9670–9679, 2015.
- [25]. A. M. Jubb, H. C. Allen, "Bisulfate Dehydration at Air/Solution Interfaces Probed by Vibrational Sum Frequency Generation Spectroscopy", *Journal of Physical Chemistry C* Vol. 116, pp. 13161–13168, 2012.
- [26]. T. I. Yacovitch, T. Wende, L. Jiang, N. Heine, G. Meijer, D. M. Neumark, K. R. Asmis, "Infrared Spectroscopy of Hydrated Bisulfate Anion Clusters: $HSO_4^-(H_2O)_{1-16}$ ", *Journal of Physical Chemistry Letter*, Vol. 2, pp. 2135–2140, 2011.
- [27]. D. E. Husar, B. Temelso, A. L. Ashworth, G. C. Shields, "Hydration of the Bisulfate Ion: Atmospheric Implications", *Journal of Physical Chemistry A*, Vol. 116, pp. 5151–5163, 2012.



- [28]. A. Kumar, A. Rani, P. Venkatesu, "A comparative study of the effects of the Hofmeister series anions of the ionic salts and ionic liquids on the stability of α -chymotrypsin", *New Journal of Chemistry*, Vol. 39, Issue 2, pp. 938-952, 2015.
- [29]. Food and Nutrition Board, Institute of Medicine of the National Academies, "*Dietary Reference Intakes for Water, Potassium, Sodium, Chloride, and Sulfate*", National academic press, pp. 424-434, 2005.
- [30]. M. Jung, W. Lee, C. Noh, A. Konovalova, G. S. Yi, S. Kim, Y. Kwon, D. Henkensmeier, "Blending polybenzimidazole with an anion exchange polymer increases the efficiency of vanadium redox flow batteries", *Journal of Membrane Science*, Vol. 580, Issue 15, pp. 110-116, 2019.
- [31]. D. Pavlov, A. Kirchev, M. Stoycheva, B. Monahov, "Influence of H_2SO_4 concentration on the mechanism of the processes and on the electrochemical activity of the Pb/PbO₂/PbSO₄ electrode", *Journal of Power Sources*, Vol. 137, Issue 2, pp. 288-308, 2004.
- [32]. C. H. VanEtten, H. L. Tookey, "*Effects of Poisonous Plants on Livestock*", Academic press, 1978.
- [33]. R. R. Nair, M. Raju, S. Bhai, I. H. Raval, S. Haldar, B. Ganguly, P. B. Chatterjee, "Estimation of bisulfate in edible plant foods, dog urine, and drugs: picomolar level detection and bio-imaging in living organisms", *Analyst*, Vol. 144, pp. 5724-5737, 2019.
- [34]. Æ. Frisch, H. P. Hratchian, R. D. Dennington II, T. A. Keith, J. Millam, "*Gauss view 05 Reference*", Gaussian, Inc., 2009.
- [35]. *Gaussian 09 manual*, <http://gaussian.com/geom/?tabid=1#GeomkeywordReadOptimization>
- [36]. Æ. Frisch, "*Gaussian 09W Reference*", Gaussian, Inc., 2009.
- [37]. Reenu, Vikas, "Exploring the role of quantum chemical descriptors in modeling acute toxicity of diverse chemicals to *Daphnia magna* Bajorath", *Journal of Molecular Graphics and Modelling*, Vol. 61, pp. 89–101, 2015.
- [38]. A. B. Marahatta, "The QSPR Studies of $[SO_4(H_2O)_n]^{2-}$, $n = 1-4$, 16 clusters through quantum-chemical descriptors", *International Journal of Progressive Sciences and Technologies*, Vol. 27, No. 2, pp. 441–454, 2021.
- [39]. G. Parr, R. G. Pearson, "Absolute hardness: companion parameter to absolute electronegativity", *Journal of American Chemical Society*, Vol. 105, No. 26, pp. 7512–7516, 1983.
- [40]. W. L. Jolly, "*Modern Inorganic Chemistry*", McGraw-Hill Book Company, New York, 1984.
- [41]. R. G. Parr, Y. Weitao, "*Density-Functional theory of Atoms and Molecules*", Oxford University Press, 1994.
- [42]. R. G. Parr, L. V. Szentpály, S. Liu, "Electrophilicity Index", *Journal of American Chemical Society*, Vol. 121, No. 9, pp. 1922–1924, 1999.
- [43]. H. Tandon, T. Chakraborty, V. Suhag, "A New Scale of the Electrophilicity Index Invoking the Force Concept and Its Application in Computing the Internuclear Bond Distance" *Journal of Structural Chemistry*, Vol. 60, pp. 1725–1734, 2019.
- [44]. J. M. J. Swanson, J. Simons, "The role of charge transfer in the structure and dynamics of the hydrated proton", *Journal of Physical Chemistry B*, Vol. 113, No. 15, pp. 5149–5161, 2009.
- [45]. E. C. Koch, "Acid-Base Interactions in Energetic Materials: I. The Hard and Soft Acids and Bases (HSAB) Principle-Insights to Reactivity and Sensitivity of Energetic Materials", *Propellants, Explosives, Pyrotechnics*, Vol. 30, No. 1, pp. 5–16, 2005.
- [46]. A. P. Kirk, T. B. Adler, H. J. Werner, "Systematically convergent basis sets for explicitly correlated wave functions: The atoms H, He, B–Ne, and Al–Ar", *Journal of Chemical Physics*, Vol. 128, No. 8, pp. 084102, 2008.

